34th Annual International Conference of the IEEE EMBS
San Diego, California USA, 28 August - 1 September, 2012

An Upper Limb Robot Model of Children Limb for Cerebral Palsy NeuroRehabilitation*

Yagna Pathak and Michelle Johnson, *Member, IEEE*

***Abstract*—Robot therapy has emerged in the last few decades as a tool to help patients with neurological injuries relearn motor tasks and improve their quality of life. The main goal of this study was to develop a simple model of the human arm for children affected with cerebral palsy (CP). The Simulink based model presented here shows a comparison for children with and without disabilities (ages 6—15) with normal and reduced range of motion in the upper limb. The model incorporates kinematic and dynamic considerations required for activities of daily living. The simulation was conducted using Matlab/Simulink and will eventually be integrated with a robotic counterpart to develop a physical robot that will provide assistance in activities of daily life (ADLs) to children with CP while also aiming to improve motor recovery.**

I. Introduction

Cerebral Palsy (CP) is a condition in which non-progressive syndromes of posture and motor impairment are displayed due to an infliction on the central nervous system (CNS) before the age of 2 years. Characteristic signs include spasticity, movement disorders, muscle weakness, ataxia, and rigidity [1]. Current therapy options include physiotherapy, orthotics, pharmacological intervention (botulinum toxin and baclofen), electric stimulation, selective dorsal rhizotomy surgery, orthopedic surgery, and spinal bracing [1-2].

Cutting-edge robotic technologies are being investigated as therapeutic options for children with CP. Ideally, a robot assisted therapy strategy must consider several factors. It should provide assistance until the child can achieve significant improvement in motor and function on ADLs, create helpful internal models that can allow users to generalize learned movements to other untrained tasks, and induce brain reorganization through interaction with the robot. The environment should motivate CP children to engage in therapeutic tasks using feedback approaches and conditioning with reward [3-6]. The MIT-MANUS, which was developed in order to investigate the clinical neurological applications of robotic therapy in stroke patients is one such system that has been successfully used to treat the upper limb impairment of children with CP. MIT-MANUS primarily moves, guides or perturbs the movement of a subject's upper limb in reaching activities [3-6]. We have developed an Activities of Daily Living Exercise Robot (ADLER) for training stroke survivors on reach and grasping tasks [3,7]. The ADLER robot was designed to train stroke subjects in real-life functional tasks that involve grasp, reach and object transportation in 2D and 3D space. The tasks included point-to-point (PTP) reaching, and functional self-care tasks like eating, drinking, combing, game-playing and household manipulation.

Our goal is to build on this previous work to develop a novel desktop robot-assisted therapy for children with CP capable of assisting bilateral and unilateral movements for reach and grasp tasks. In order to do this, we first sought to develop a general robot model that can describe kinematic and dynamic features of the healthy and impaired movement for children with and without CP. Studies on movement kinematics of children with CP can inform this model. For example, Mackey [2] explored the differences in 3D kinematics between control children versus CP children on real activities. Tasks included a hand-to-head, hand-to-mouth, and a reach movement. His results indicate that hemiplegic children are significantly slower than control children in task completion with reduced range of motion or shifted maximum and/or minimum. Therefore, an accurate robot model is needed to simulate these attributes. In addition, recovery studies demonstrate that improved reaching kinematics can be defined by improved smoothness and improved time [5,6].

A simple mathematical model of the upper limb can be used to assess the level of disability and assist in determining the effectiveness of robotic therapy. Most mathematical models must consist of forward and inverse kinematics, forward and inverse dynamics and corresponding control laws. While the methods for deriving the forward kinematic parameters are well-developed using Denavit-Hartenburg parameters [9], there are various gaps in choosing an ideal method to model the inverse kinematics and the dynamics of a complex manipulator [9-12]. For example, Kamper and Rymer [10] used the Levenberg-Marquardt method to derive inverse kinematics. They modeled the workspace of the human arm (5 DOF) while examining the interdependence of position and orientation from a geometric perspective. They noted that physiological limits in joint ranges due to impairment can decrease size of the reach loci and the amount of redundancy in the human arm. Abdel-Malek offers a closed-form solution for the inverse kinematics [11]. This method takes into account physiological joint limits and identifies barriers that a person may encounter to attain a different posture. These barriers are modeled as imaginary surfaces in this algorithm and singularities are explicitly modeled. Ali and colleagues suggested another closed-form approach [12] for a humanoid robot and utilized a new reverse decoupling method that relied on viewing the upper limb kinematic chain in reverse order. The equations for deriving the joint angles are solved by using the known position and

*Research supported by Department of Physical Medicine and Rehabilitation, Medical College of Wisconsin (MCW), National Institutes of Health Career Award K25NS058577-1A04 and RERC Technologies for Children with Orthopedic Disabilities: US Department of Education, H133E100007

Y Pathak is with Biomedical Engineering, Marquette University, Milwaukee, WI USA (e-mail: yagna.pathak@ marquette.edu).

M. J. Johnson is also with Physical Medicine and Rehabilitation, MCW and Biomedical Engineering, Marquette University, Milwaukee, WI USA. (Corresponding author: e-mail: mjjohnso@mcw.edu).

orientation of the hand with respect to the shoulder. Our approach utilizes this technique to define the inverse kinematics. The procedures to derive dynamics used the approached outlined by Niku and colleagues and standard parameters for defining human forearm, upper arm and hand [8,13-15]. Values for segment mass, radius of gyration and center of mass specifically for children are scarce. Mass parameter ratios provided by Winter et al. are often used [13].

This paper describes the 6-DOF kinematic and dynamic model of the upper arm of children with and without CP. We present the workspace of a healthy versus a CP child movement and the kinematics and dynamics results for a simple PTP reaching task as described by Mackey involving reach from a table-top to a target positioned at a distance on the trunk's midline.

II. METHOD

A. Kinematic Analysis

In order to create and simulate a mathematical model of the upper limb in CP subjects, a 3DOF shoulder (flexion and extension, θ_1, abduction and adduction, θ_2, internal and external rotation, θ_3), a 2DOF elbow (flexion and extension, θ_4 and pronation supination, θ_5) and a 1DOF wrist (flexion and extension, θ_6) were modeled. The frame assignments at each joint are shown below in Figure 1. The joint angles, θ_i revolves around Z_{i-1} as indicated in Figure 1 and Table1. Table 2 summarizes the D-H parameters that were used to calculate the A-matrices that describe rotation and translation from one joint to the next. The homogenous transform (T-matrix) was used to extract the position and orientation matrices that represent the end-effector (hand) with respect to base frame (Equation 1) [8].

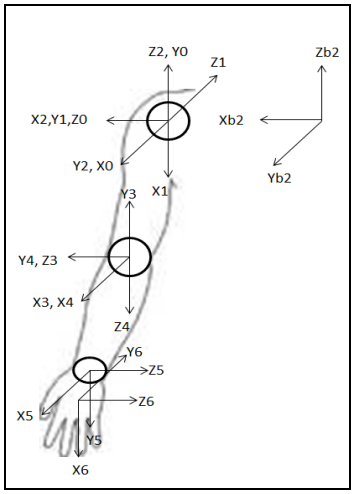

Figure 1: Denavit-Hartenburg (D-H) Frame Assignment for the Upper Arm model [8]

The forward kinematics equations were then identified with the vector, *p*. The position vector to the wrist is given by p_{wrist} in Equation 2. The position of the hand is derived using Equation 3 and 4. The simulations were conducted in MATLAB with the use of symbolic toolbox and 3D graphics. Both 2D and 3D simulations were conducted and the workspace was analyzed for healthy versus CP children. The ROM for the joints was reduced to 70% [12] of the normal range to simulate pathological conditions.

TABLE I
JOINT RANGE OF MOTION PARAMETERS
(IMPAIRMENT IS MODELED AS 70% REDUCTION IN ROM.)

Joints (i)	**Healthy-ROM degrees (radians)**
Shoulder adduction/ abduction	-70 to 70° (-1.22 to 1.22)
Shoulder flexion/ extension	-69.6 to 169° (-1.21to 2.95)
Shoulder medial /lateral rotation	-184.7 to 107.4° (-3.24 to1.845)
Elbow flexion/ extension	-2.1 to 146.5° (-0.04 to2.56)
Elbow pronation/ supination	-76.9 to 82.9° (-1.34 to 1.45)
Wrist flexion/ extension	-70 to 70° (-1.22 to 1.22)

TABLE II
D-H PARAMETERS

	θ	a meters	α radians	d meters
A_1	θ_1	0	π/2	0
A_2	θ_2	0	- π/2	0
A_3	θ_3	0	π/2	l_1=0.17
A_4	θ_4	0	π/2	0
A_5	θ_5	0	π/2	l_2=0.27
A_6	θ_6	l_3=0.19	0	0

According to Pieper, a closed-form inverse kinematic solution for a manipulator can be achieved if three adjacent axes intersect at a single point or if three adjacent axes are parallel. Because our model uses a 3DOF shoulder, the whole arm can be modeled in reverse order to extract the joint positions. The end-effector becomes the base and leads to the inverse homogeneous transform matrix (T'=inv(T_6)) in terms of ${}^6A_0$ [12]. The symbolic implementation of this method can be achieved by using arctan. In the extensive explanation of this method provided by Ali et al., a decision making process is described to choose between multiple solutions. Also, conditional loops are incorporated in the MATLAB code to account for singularities.

$$T_5 = A_1 A_2 A_3 A_4 A_5 = \begin{bmatrix} {}^0_5R & {}^0_5p = p_{wrist} \\ 000 & 1 \end{bmatrix} \quad (1)$$

$$p_{wrist} = \begin{bmatrix} l_1 c_1 s_2 - l_2(s_4 s_1 s_3 - s_4 c_1 c_2 c_3 - c_4 c_1 s_2) \\ l_1 s_1 s_2 + l_2(s_4 c_1 c_3 + s_4 s_1 c_2 c_3 + c_4 s_1 s_2) \\ -l_1 c_2 - l_2(c_2 c_4 - c_3 s_2 s_4) \end{bmatrix} \quad (2)$$

$$T_6 = A_1 A_2 A_3 A_4 A_5 A_6 = \begin{bmatrix} {}^0_6R & {}^0_6p \\ 000 & 1 \end{bmatrix} \quad (3)$$

$${}^0_6p = p_{hand} = p_{wrist} + {}^0_6R \begin{bmatrix} 0 \\ 0 \\ l_3 \end{bmatrix} \quad (4)$$

TABLE III
LINK PARAMETERS

Link (i)	Mass (m_i) kg	Length (l_i) meters	Radius (r_i) meters
Shoulder to Elbow ($i=1$)	0.767	0.168	0.0429
Elbow to Wrist ($i=2$)	0.438	0.273	0.0233
Wrist to Hand ($i=3$)	0.164	0.191	0.0308

B. Dynamic Analysis

The dynamics were evaluated by using a computational method that can be used with MATLAB described in Niku and colleagues [8]. In order to derive each element (D_{ij} or D_{ijk}) of the mass-inertia, centrifugal and coriolis matrix, certain coefficients (U_{ij} and U_{ij}) were calculated (see Equations 5-7). The J-matrix in these equations refers to the pseudo-inertia matrix (Equation 8). To obtain the moments of inertia each link was modeled as a regular solid cylinder. Equations 9 and 10 were used for links i=1 and i=2 and Equations 11 and 12 were used for link 3. These were calculated at the joint using the parallel axis theorem and center of mass location were derived based on assumptions in [13, 14] about the location of the center mass with respect to the link length. These locations were $l_{cm1} = 0.436 l_1$, $l_{cm2} = 0.43 l_2$, and $l_{cm3} = 0.43 l_3$. These equations were used to derive equations of motion for the model (Equation 11). The mass, length and radius are detailed in Table III.

$$\frac{\partial T_i}{\partial q_j} = U_{ij} = A_1 A_2 Q_j A_j A_i \quad \text{and} \quad U_{ijk} = \frac{\partial U_{ij}}{\partial q_k} \quad (5)$$

$$D_{ij} = \sum_{p=\max(i,j)}^{n} Trace\ (U_{pj} J_p U_{pi}^T) \quad (6)$$

$$D_{ijk} = \sum_{p=\max(i,j,k)}^{n} Trace\ (U_{pjk} J_p U_{pi}^T) \quad (7)$$

$$J_i = \begin{bmatrix} \frac{I_{xx} + I_{yy} + I_{zz}}{2} & I_{xy} & I_{xz} & m_i x_i \\ I_{xy} & \frac{I_{xx} - I_{yy} + I_{zz}}{2} & I_{yz} & m_i y_i \\ I_{xz} & I_{yz} & \frac{I_{xx} + I_{yy} - I_{zz}}{2} & m_i z_i \\ m_i x_i & m_i y_i & m_i z_i & m_i \end{bmatrix} \quad (8)$$

$$I_{xx} = I_{yy} = \frac{1}{12} m_i (3 r_i^2 + l_i^2) + m_i l_{cmi}^2 \quad (9)$$

$$I_{zz} = \frac{1}{2} m_i r_i^2 + m_i l_{cmi}^2 \quad (10)$$

$$I_{yy3} = \frac{1}{12} m_3 (3 r_3^2 + l_3^2) + m_i l_{cm3}^2 \quad (11)$$

$$I_{z3} = I_{xx3} = \frac{1}{2} m_i r_3^2 + m_i l_{cm3}^2 \quad (12)$$

$$\tau = B\ddot{q} + C(q, \dot{q}) + G(q) \quad (13)$$

C. Simulation

The simulation was created on Matlab/Simulink. The model was modified from the original version created by Formica et al [14]. Modifications were made to implement the human arm in 3D versus 2D as it was initially modeled. Also, the human arm was now modeled in a more realistic manner with 6DOFs. Several assumptions were made in order to simplify the mathematics. The shoulder position (0, -0.9144, 0.1579) is defined in Cartesian-base coordinate system which was then used for the entire simulation. The inverse kinematics and dynamics modules were also changed to incorporate the methods described here. This was done in an effort to implement closed-form approaches that can provide a solution that is more accurate. The simulation duration was set to 3.0 seconds. It was used to extract information about Cartesian and joint positions and velocities, trajectory patterns, torques, and forces. The results for these are presented below. The movement executed by the simulation is the PTP reaching movement described by Mackey [2]. The initial position is (-0.1529,-0.4232, -0.4432) in which the hand is resting on the table-top and the final position is (0,-0.282,0.157), a point directly across the shoulder. The workspace results for both groups were calculated using the ROM for each joint as shown in Tables 1 and 2. The link-lengths are anthropomorphic values listed in previous literature (see Table 3). The normalized path plan algorithm used was the quintic polynomial [8]. The impaired user was also modeled as being unable to move along a straight line path (Dis = 1 and Dis 2) to account for quantization of the movement with increasing pathology [14]. The equivalent joint angles were derived.

III. RESULTS

The top panel of Figure 2 shows the workspace results after moving the model through the healthy (larger child) and reduced ranges of motion in XY and XZ directions. The position of the hand is shown. As expected, the workspaces for CP children are far smaller than those of healthy subjects. The lower panel of Figure 2 shows the target movement plan for robot model. Figure 2c shows the XYZ plot of the plan. Figure 3 shows the shoulder flexion/extension joint motions results from the simulation.

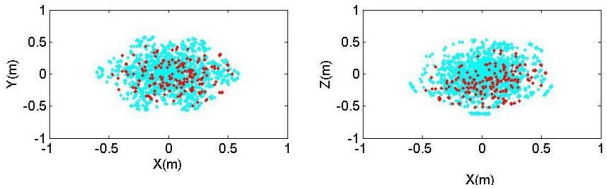

Figure 2ab: Top: Workspace of healthy (left) versus CP (right) children in 2D assuming 70% decrease in ROM for CP Bottom.

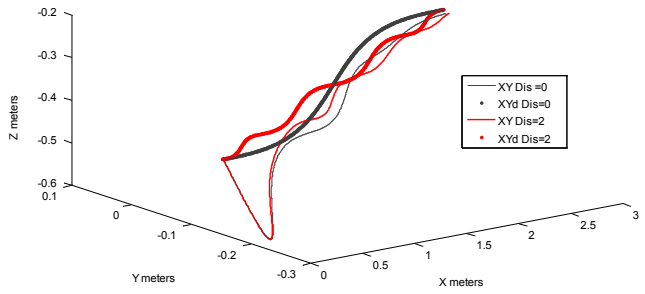

Figure 2b: XYZ path point for Dis=0 and Dis=2 planned and resulting fromsimulation.

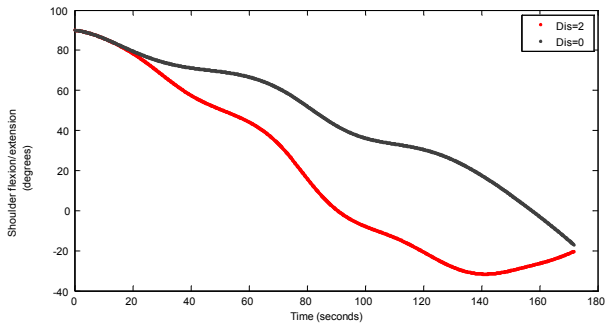

Figure 3: Shoulder flexion and extension in degrees generated based on disability level from the simulation. Dis = 0 (control) and Dis =2 (cp)

IV. Discussion and Conclusions

As expected since we assumed that the range of motion was reduced, the workspace of CP children is much smaller than that of control subjects. While the therapy program may start by assisting a child whose workspace closely resembles that of the one shown for CP subjects, the eventual goal of these therapies will be to help these children attain increasingly normal workspaces to carry out ADLs in a more effective manner. The equivalent joint angles for the path plan resolved to the joint angles. The plan gave dissimilar joint results as compared to Mackey [2]. Mackey results indicated that CP children should move slower than control; a range of 4.0 to 7.0sec versus 2.4 to 3.4sec for reach task. They plotted shoulder and elbow flexion with and without CP. They observed that shoulder flexion (min: 20±14 and max: 94±13). Our model predicted shoulder flexion/extension minimum and maximum to be of similar range but we expected the movement would go from smaller to larger joint angles. These results suggest that model needs to be improved.

We predict much higher torque-profile and force-profile for CP children than for normal children. This is because there is definite evidence that CP subjects have an impaired sense of force coordination. The torque profiles for each condition will be increasingly perturbed as the disability worsens. This implies that CP children are unable to control forces and torques that are required for task completion.

Robot technology has an increasing necessity in the field of CP therapy to help recover motor function. Therapy that focuses on brain-plasticity and implements relevant task training will tend to be most effective. While most of the current technologies are directed toward stroke survivors, alterations and improvements to these can lead to technologies that will help the CP population. In order to create effective robotic therapies, it is essential to develop usable and simple models that can provide insight into the subject's level of disability and the type of assistance required. Our results show a step forward in this direction, but does need some re-design.

Acknowledgment

We thank Dr. D. Formica and Dr. E.Gugliemelli for providing the MIT –MANUS simulation modeled edited for this model.

References

[1] Koman, Paterson A, Smith B, Shilt, J. Cerebral Palsy. The Lancet, Vol. 363: 1619-1631.

[2] Mackey A, Walt S, Stott S. Deficits in Upper-limb Task Performance in Children with hemiplegic Cerebral Palsy as defined by 3-Dimensional Kinematics. Arch Phys Med Rehabil, 2006, 87: 207-215.

[3] Timmermans, Annick, et al. Technology-assisted training of arm-hand skills in stroke: concepts on reacquisition of motor control and therapist guidelines for rehabilitation technology design. 2009, Biomed Central.

[4] Fluet G, Qiu Q, Kelly D, Parikh H, Ramires D, Saleh S, Adamovich S. Interfacing a haptic robotic system with complex virtual environments to treat impaired upper extremity motor function in children with Cerebral Palsy. Dev. Neurorehabilitation, 2010; 13: 335-345.

[5] Fasoli SE, Fragala-Pinkham M, Hughes R, Hogan N, Krebs HI, Stein J. Upper limb robotic therapy for children with hemiplegia. Am J Phys Med Rehabil 2008; 87: 929–36.

[6] Krebs HI, Volpe BT, Williams D, *et al.* Robot-aided neurorehabilitation: a robot for wrist rehabilitation. IEEE Trans Neural Syst Rehabil Eng 2007; 15: 327–35.

[7] Johnson MJ, Wisneski K, Anderson J, Nathan DE, Strachota E, et al. Task-oriented and Purposeful Robot-Assisted Johnson MJ Therapy, In Rehabilitation Robotics, Editor, A. Lazinica, International Journal of Advanced Robotics Systems, Vienna, Austria, 2007, ISBN 978-3-902613-04-02

[8] Niku, Saeed. Introduction to Robotics: Analysis, Systems, Applications.

[9] Kamper D, Rymer Z. Effects of geometric joint constraints on the selection of final arm posture during reaching: a simulation studys.l. : Exp Brain Res, 1999;126: 134-138.

[10] Abdel-Malek, Karim, et al Towards understanding the workspace of human limbs.. 13, s.l. : Ergonomics, 2004; 47: 1386-1405.

[11] Ali MA, Park HA, Lee CSG. Closed-Form Inverse Kinematic Joint Solution for Humanoid Robots. 2010, Intelligent Robots and Systems (IROS), IEEE/RSJ International Conference, 2010; 704-709.

[12] Winter, D.A. Biomechanics and Motor Control. 2. s.l. : University of Waterloo Press, 1992.

[13] Clauser, Charles. Weight, Volume, and Center of mass of segments of the Human Body. 1969, Air Force Systems Command.

Formica D, Zollo L, Guglielmelli E, Torque-Dependent Compliance Control in the Joint Space for Robot-Mediated Motor Therapy. J. Dyn. Sys., Meas., Control 128, 152 (2006).